

In presenting this thesis in partial fulfillment of the requirements for an advanced degree at Idaho State University, I agree that the Library shall make it freely available for inspection. I further state that permission for extensive copying of my thesis for scholarly purposes may be granted by the Dean of the Graduate School, Dean of my academic division, or by the University Librarian. It is understood that any copying or publication of this thesis for financial gain shall not be allowed without my written permission.

Signature _____

Date _____

Comparison of Filter Media Collection Efficiency for Environmental

Monitoring using Be-7 as a Challenge Aerosol

by

Jose Hurtado

A thesis

submitted in partial fulfillment

of the requirements for the degree of

Master of Science in the Department of Physics

Idaho State University

Fall 2018

To the Graduate Faculty:

The members of the committee appointed to examine the thesis of Jose Hurtado find it satisfactory and recommend that it is accepted.

Dr. Rich Brey,
Major Advisor

Dr. Thomas F. Gesell,
Committee Member

Dr. DeWayne Derryberry,
Graduate Faculty Representative

Acknowledgements

To my Player 2, without whom this would not be possible. Thank you to Dr. Rich Brey, my advisor, for taking a chance and allowing me the opportunity to pursue my ambitions. A special thanks to Roy Dunker for helping me shape this idea and showing me the ropes. To Paul Ritter and Celena Lewis, thank you for all your assistance in obtaining data and the use of your equipment. Thanks to Kevin Claver for being there to help me formulate my thoughts and teaching me how to write. Hooyah, Navy!

TABLE OF CONTENTS

LIST OF FIGURES.....	v
LIST OF TABLES.....	vi
ABBREVIATIONS	vii
ABSTRACT.....	viii
Chapter 1: INTRODUCTION.....	2
1.1 Idaho DEQ.....	2
1.2 Monitoring Issue.....	3
1.3 Proposed Experiments.....	6
1.3.1 Experiment I.....	6
1.3.2 Experiment II.....	7
1.3.3 Experiment III.....	8
Chapter 2: LITERATURE REVIEW.....	9
2.1 Worldwide Beryllium 7	9
2.2 Beryllium-7 Production.....	10
2.3 Beryllium-7 Dispersion and Deposition.....	11
2.4 Beryllium 7 Particle Size Distribution.....	12
2.5 Snake River Plains Be-7.....	14
2.6 Idaho DEQ Sampling Equipment.....	18
2.7 Filter Nomenclature Designation.....	20
2.8 Particle Collection media.....	20
2.9 7-Stage Cascade Impactor.....	25
2.10 High Purity Germanium Gamma Spectroscopy.....	27
2.10.1 Semi-conductor detectors.....	27
2.10.2 Detector calibrations.....	30
Chapter 3: METHODS AND MATERIALS.....	32
3.1 Materials.....	32
3.2 Experiment I: Side-by-side filter collection efficiency comparison.....	33

3.2.1 HP(Ge) calibration.....	33
3.2.2 Obtaining the samples.....	34
3.2.3 Analyzing the samples.....	35
3.2.4 Filters in series.....	35
3.3 Experiment II: Particle size distribution of the 5- μm filter.....	37
3.4 Experiment III: Filter recount as a composite.....	39
Chapter 4: RESULTS AND DISCUSSIONS	40
4.1 Experiment I: Side-by-side filter collection efficiency comparison.....	40
4.1.1 Filters in series.....	41
4.2 Experiment II: Particle size distribution of the 5- μm filter.....	42
4.3 Experiment III: Filter recount as a composite.....	44
Chapter 5: CONCLUSIONS AND FUTURE WORK.....	45
REFERENCES.....	46
APPENDIX.....	48

LIST OF FIGURES

Figure 1: Be-7 production to analysis block diagram.....	5
Figure 2: Proposed 5- μm particle sizing experiment illustration	7
Figure 3: AMAD distribution of Be-7 ambient aerosols.....	13
Figure 4: Snake River Plains Sampling Locations.....	15
Figure 5: Chart of reported Be-7 values from Idaho DEQ for the Snake River Plains.	16
Figure 6: Sunspot activity during solar cycle 22 and 23.....	17
Figure 7: Electron microscope image of Versapor® acrylic Copolymer Membrane Disc Filter..	21
Figure 8: Aerosol particle collection mechanisms.....	24
Figure 9: Aerosol particle collection mechanism efficiencies.....	25
Figure 10: Cross-sectional view of the 7-stage cascade impactor.....	26
Figure 11: Electron energy requirements of insulators and semi-conductors.....	27
Figure 12: P-type acceptor site.....	28
Figure 13: Depleted region and reverse bias.....	29
Figure 14: HP(Ge) detector and cryo-unit construction.....	30
Figure 15: Cs-137 full-energy peak assigned to channel.....	31
Figure 16: Series sampling apparatus.....	37
Figure 17: Versapor-5000® 5- μm filter in an aluminum sampling cartridge.....	38
Figure 18: Experiment III final sampling setup.....	39

LIST OF TABLES

2.1 Sampling location latitudes and elevations.....	15
4.1 Idaho Falls side-by-side sampling results.....	41
4.2 5- μm and 3- μm in-series samples.....	42
4.3 Cascade impactor mass by stage.....	43
4.4 Single filter activity versus composite recount activity.....	45

ABBREVIATIONS

Be-7 – Beryllium 7

DEQ – Department of Environmental Quality

INL – Idaho National Laboratory

HP(Ge) – High purity germanium

GCR – Galactic Cosmic Rays

Ci – Curies

pCi – pico curies (1×10^{-12} Curies)

fCi – femto curies (1×10^{-15} Curies)

m³ – cubic meter

mm - millimeters

μm – micrometer/micron

eV – electron volt

CFM – cubic feet per minute

LCD – liquid crystal display

PLC – programmable logic controller

TSP – total suspended particulate

MDA – minimum detectable activity

Comparison of Filter Media Collection Efficiency for Environmental
Monitoring using Be-7 as a Challenge Aerosol

Thesis Abstract—Idaho State University (2018)

The purpose of this study was to field test the Versapor-5000® 5- μm filter and the Versapor-3000® 3- μm filter and compare atmospheric radionuclides collection efficacy. A side-by-side direct comparison was conducted, resulting in an average collection efficiency of Be-7 aerosols by the 5- μm filter of $78.9 \pm 12.6\%$ of that collected by the 3- μm filter. A series-sample experiment resulted in $12.8 \pm 7.2\%$ of Be-7 activity passing through the 5- μm filter and collected by the 3- μm filter. The normal laboratory method of determining Be-7 concentrations is to analyze a quarterly composite of 13 samples. Each filter was analyzed on the detector face and again on a stack on 12 unused copolymer membrane filters, where approximately $13.3 \pm 3.6\%$ of the calculated Be-7 activity was lost. A 7-stage cascade impactor showed the 5- μm filter has a 100% collection efficiency of particles 1.0- μm and larger; 88.6% of the uncollected particles were $\leq 0.6\text{-}\mu\text{m}$.

Keywords: Beryllium 7, Be-7, environmental air monitoring, DEQ

Chapter 1: INTRODUCTION

1.1 Idaho DEQ

The Idaho Department of Environmental Quality (DEQ) Idaho National Laboratory (INL) Oversight Program measures the concentration of radioactive materials in air at eleven locations around the INL site. The measurements around INL provide a baseline of regional ambient air concentrations of naturally occurring radionuclides and the means to identify and quantify concentrations of airborne radioactivity caused by emissions from the INL or other sources.

The current method of sampling is a weekly continuous sample using the Hi-Q¹ 3-stage, brushless, automatic flow control, outdoor 4-inch diameter high volume air sampler for continuous use. Filters are changed out weekly, usually every Thursday after sampling for the entirety of the 168-hour week. The samples are delivered to Idaho State University's Environmental Monitoring Lab on the following Monday where gross alpha and beta counts are performed on Tuesday, five days after collection. The five-day delay allows the short-lived natural radionuclides to decay to insignificance. The filters are then stored for a quarterly composite gamma spectroscopy analysis that, among other things, measures the concentration of Beryllium-7. Current filter media is a Versapor-3000® acrylic copolymer membrane on a nonwoven nylon support with a pore size of 3 microns (3- μm).

The 4-inch filters are separated by location and stapled together when prepared for the quarterly gamma spectroscopy analysis. The filters are stacked in chronological ascending order and placed in a plastic cylindrical holder with a diameter slightly larger than 4 inches, thus

¹ Hi-Q Environmental Products Company. 7386 Trade St. San Diego, CA 92121

producing consistent placement of the samples near the high purity Germanium HP(Ge) detector. The filters are analyzed for 16.6 hrs (1,000 min).

Samples are decay corrected to the time of collection and activity is reported in units of picocuries (pCi) per sample. The total volume of air sampled is logged during the weekly changeouts by DEQ employees in cubic meters. The activity concentrations of Be-7 are determined in units of picocuries per cubic meter (pCi/m³). The samplers are set to draw air at 6 standard cubic feet per minute (scfm or cfm).

1.2 Be-7 Monitoring Issue

An experiment was conducted during the 3rd quarter of 2016. Samples for the quarter for one Idaho Falls sample location were analyzed on a weekly basis by HP(Ge) gamma spectroscopy for Be-7 activity. The weekly Be-7 concentrations were in the range of 1.46×10^{-2} to 1.39×10^{-1} pCi/m³ with an average of 6.75×10^{-2} pCi/m³.

The same OP163IHR 3rd quarter 2016 samples were counted again as a 13-week quarterly composite to complete the normal DEQ contracted analysis, with a reported Be-7 activity concentration of 5.61×10^{-2} pCi/m³. The total activity of the filters was 1,327.6 pCi. The total summed activity of each of the weekly filters after decay correcting was 1,677.32 pCi. The composite count total activity resulted in a 20.8% deviance from the individual counts. Why the difference?

One possible explanation for the activity variance is volume sampled; the week of 10/6 through 10/13 had a sample volume of 350 m³. A typical 168 hours of continuous sampling should result in a total volume sampled of 1,711 m³/week at a rate of 6 cfm. A lower total volume sampled

does not completely negate the data since the activity is reported in picocuries per cubic meter (pCi/m^3), however this does increase uncertainty in sampling and subsequently in the final propagated error in the reported value.

Another possible cause is the two gamma spectroscopy analysis methods used to count the air filters. Each weekly filter counted during the experiment was placed at the closest distance possible to the detector face when counted individually. The quarterly composite counts are stacked and stapled together, resulting in 12 additional filters that are not at the same distance relative to the distance when counted individually. The same detector efficiency and geometry calibration were used for both methods, but this did not factor in the distance created between the detector face and the stacked filters.

The purpose of this thesis is to analyze each step in the process of creating, sampling, and analyzing natural Be-7 and determine the cause of such a large deviance in activity concentrations. A statistical analysis of the reported concentrations locally in the Snake River Plains was conducted and compared to reported results from locations world-wide. The following is a simple block diagram of the events that occur in the environmental monitoring process:

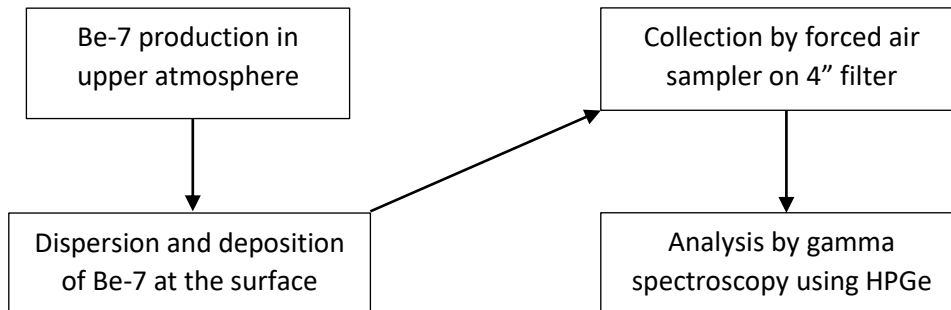


Figure 1. Block diagram of Be-7 production to analysis.

1.3 Experiments and Hypotheses

1.3.1 Experiment I: Perform a side-by-side comparison of filter collection efficiencies using a 5- μm Versapor-5000® filter and a 3- μm Versapor-3000® filter. Each filter will then be counted on the same ORTEC 100% relative efficiency, Gem-Top HP(Ge) detector to determine activity of Be-7 using the 477-keV gamma emission with 10.85% yield. The experiment was performed three times over three weeks to gather sufficient data to extrapolate a trend and a conclusion.

Ho: The Versapor-5000® 5- μm filter in comparison with the Versapor-3000® 3- μm filter is able to collect the same amount of Be-7 activity from the atmosphere.

Ha: The Versapor-5000® 5- μm filter in comparison with the Versapor-3000® 3- μm filter is not able to collect the same amount of Be-7 activity from the atmosphere.

If the activity concentrations determined by the Versapor-5000® are within 5% and does not show a consistently lower concentration than that of the Versapor-3000®, the evidence would suggest an adequate efficacy of the 5- μm filter. A conversion to the 5- μm filter would allow the samplers to perform with less flow restriction based on filter pore size.

1.3.2 Experiment II: Draw an air sample through a 5- μm filter for particle collection efficiency. A cascade impactor will be placed in-line immediately after the filter apparatus to collect and characterize the size of the particles not collected by the filter. Forced air flow through the filter and cascade impactor is initiated by a vacuum pump and flow rate is controlled by a graduated rotameter with a flow valve control. The following block diagram illustrates the setup of the equipment used to conduct the experiment:

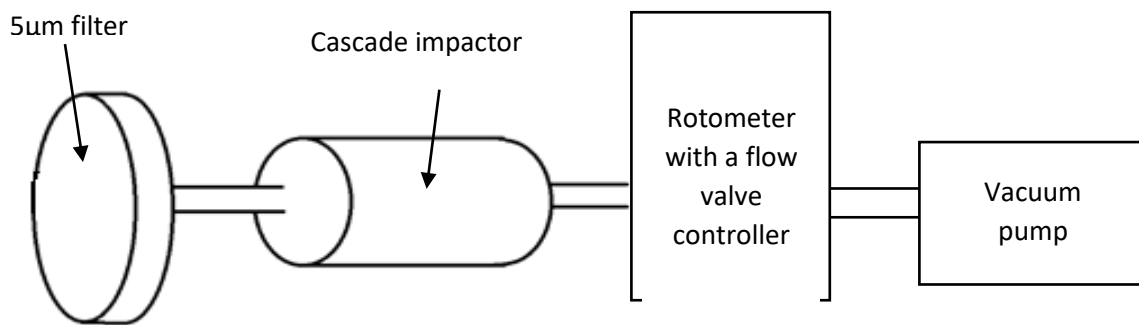


Figure 2. Proposed 5- μm particle sizing experiment construct.

Ho: The 5- μm filter collects particle sizes small enough to accurately measure Be-7 concentrations.

Ha: The 5- μm filter does not collect particle sizes small enough to accurately measure Be-7 concentrations.

Be-7 attaches to particles as small as 0.4- μm in diameter (Sec 2.4, Figure 3). The cascade impactor will determine the size distribution of the particles not collected by the 5- μm filter.

1.3.3 Experiment III: Perform gamma analysis on one normal weekly filter. Re-perform Be-7 activity analysis on the same sample stacked on 12 non-used copolymer membrane filters and compare to the calculated activity of the single filter. The stack of filters simulates the quarterly composite method. The experiment would suggest a loss of efficiency in measuring activity when counted as a composite due to distance, self-shielding of emitted photons or a combination of both.

Ho: The measured activity of the stack of filters is consistent with the measured activity of the single filter.

Ha: The measured activity of the stack of filters is less than the measured activity of the single filter.

Chapter 2: Literature Review

2.1 Worldwide Be-7

Be-7 surface air concentrations have been reported from numerous latitudes and altitudes worldwide since 1955. Some of the first reports of Be-7 detection in the literature were by laboratories in Chicago, IL from rainwater samples collected in Lafayette, IN during 1953 and 1954. In 1956, the first detection of Be-7 in aerosol particles was made and quantification of concentrations has since ensued. (Doering 2007)

There are inherent obstacles in quantifying Be-7 surface air concentrations due to the many factors involved when determining accuracy of analysis. Data from a single location should not be directly compared to 60 years of world-wide data in search of a trend. Production rates of Be-7, residence time in the atmosphere, precipitation and washout, chronological progression of solar cycle, seasonal variabilities, collection methods and materials, detection methods and materials, and the occasional human error pose a multi-variable complexity to accurately depict the behavior of Be-7.

Seasonal variation of Be-7 surface concentrations, in general, can be attributed to the exchange rate of air between the troposphere and the stratosphere as discussed further in section 2.3. Middle latitudes exhibit intra-tropospheric mixing during the warmer months. Higher latitudes gain Be-7 from the lower latitudes due to air mass transport towards the poles (Feely 1989).

The highest concentration found in literature was in Salt Lake City, UT from the years of 1971 to 1975 the August mean concentration was 260 fCi/m³. The lowest concentration reports found in the literature was Barrow, AK from the years of 1975 to 1985, the August mean

concentration was 18 fCi/m³ (Feely 1989). These reported values illustrate the variability of Be-7 concentrations as they were during the same seasonal time-frame of August during the solar activity minimum, in the midst of the transitional period between solar cycle 20 and 21.

2.2 Beryllium 7 Production

Beryllium-7 is a naturally occurring radioisotope of Beryllium created in the Earth's upper atmosphere by cosmic rays. The primary cosmic ray flux that interacts with the Earth's atmosphere is composed of Galactic Cosmic Rays (GCR), which are high-energy particles originating outside of the solar system as well as lower-energy particles emitted by the sun (Talpos 2005, Kotsopoulou 2010). GCR flux is consistent to within 10% and the evidence suggests it has not changed for at least the last few million years (Kotsopoulou 2012). In contrast, solar emissions fluctuate constantly throughout an 11-year cycle and peak with events such as coronal mass ejections producing solar flares and intense particle flux.

Cosmic rays are primarily high-energy electrons, protons and alpha particles that induce nuclear spallation in the upper troposphere and lower stratosphere. Nuclear spallation is a process by which a cosmic proton, neutron, or light nucleus with the kinetic energy of about 10⁹ eV interacts with a heavy nucleus, typically Oxygen, Nitrogen and Argon, causing the emission of a spectrum of energetic particles and fragments of the original atom (Rez 2010), including Be-7.

The production rate of Be-7 is inversely proportional to the 11-year solar cycle; when the magnetic field and solar activity are at maxima, the production of Be-7 is at its lowest in the cycle (Jiwan 2013). GCR and solar emissions are competing sources of cosmic rays that interact with the atmosphere. Solar particles have energies in the range of 10³ eV to 10⁸ eV and a fluctuating

flux. GCR have energies in the range of 10^6 eV to 10^{20} eV and much lower albeit consistent flux. During a time of solar activity minima, GCR then becomes a greater percentage of the cosmic ray interactions and due to the higher energies will induce more spallation reactions, thus increasing the production of Be-7. During times of high solar activity, the sun's magnetic field will strengthen and deflect cosmic rays away from the solar system resulting in a decrease of the Be-7 production rate (Talpos 2005).

Be-7 is predominantly produced in the lower stratosphere and upper troposphere; approximately two thirds of Be-7 produced is created in the stratosphere due to atmospheric attenuation (Talpos 2005). Earth's magnetic field also affects Be-7 production as it directs the energetically charged cosmic particles to the poles thereby increasing the production through spallation at the poles and decreasing the production as latitude approaches the equator.

Be-7 has a half-life of 53.3 days and decays by electron capture to Li-7 (Terzi, Kalinowski 2017). Be-7 is the lightest radionuclide that decays exclusively through electron capture. Be-7 has an affinity for Oxygen bonding creating BeO or BeOH where it then attaches to aerosols. The greatest percentage of the aerosolized Beryllium is in the range of 0.4 to 1.2 micrometer (μm) making them subject to traveling with seasonally determined air flows (Jiwan 2013).

2.3 Be-7 Dispersion and Deposition

The concentration of Be-7 detected at the surface, regardless of altitude, has a seasonal pattern with maximum values in the spring and summer and minimum values in the fall and winter.

The incorporation of Be-7 into the lower layers of the troposphere is due to the displacement of masses of air from higher layers caused by solar radiation. The maximum values

of Be-7 concentrations in the hottest months may be understood by considering vertical air mixing. The rising hot air forces the cold air in the higher layers, where there are greater concentrations of cosmogenic radionuclides, to move downwards. The heating of air masses is directly related to the longer length of the solar day and the greater angle of incidence of solar radiation during the summer (Bas 2016).

The fate of Be-7 is inevitably the fate of the carrier aerosols. Considerable coagulation occurs during the migration from the stratosphere and upper troposphere to the ground. Mean tropospheric residence times have a reported global average of 21 days. However this value decreases to an average of 10 to 15 days due to washout in regions of higher precipitation. Dry areas and Polar Regions report an average residence time of 25 to 40 days.

2.4 Be-7 particle size distribution

Beryllium-7 attaches primarily to particles in the atmosphere that have an Activity Median Aerodynamic Diameter (AMAD) between 0.4 μ m to 1.6 μ m. It has been observed that 83% of the atmospheric Be-7 is associated with particles smaller than 1.1 μ m. The following diagram illustrates the particle distribution reported in a study conducted in Thessaloniki, Greece from 21 November 1991 to 22 June 1993:

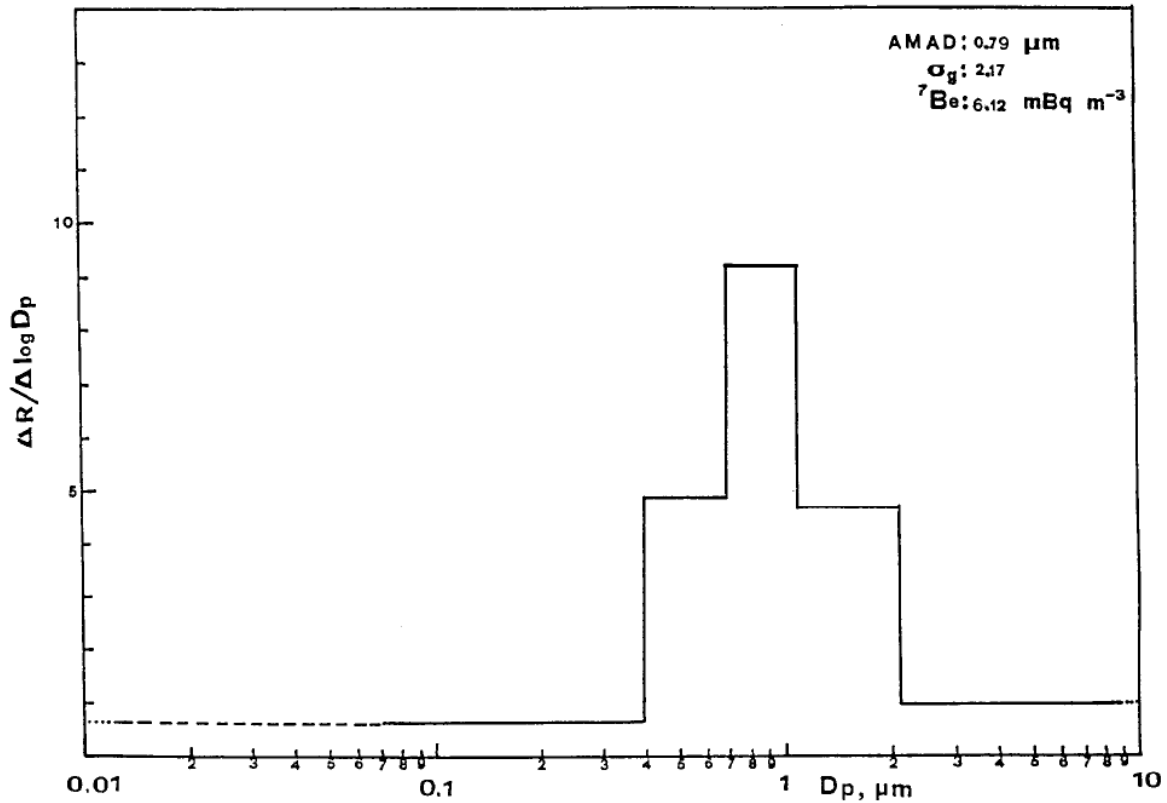


Figure 3. AMAD distribution of Be-7 ambient aerosols (Papastefanou 1996)

In the presence of pollutants, Be-7 attaches to larger particles which shifts the size distributions. During the production stage in the upper atmosphere, Be-7 is initially in atomic form. As Be-7 electrostatically attaches to materials, molecular coagulation occurs allowing for the settling into denser atmospheric layers. Each atmospheric layer has characteristic wind patterns and size distribution of particulates. In a dry, arid location, smaller particulate in the submicron size are able to settle on the Earth's surface shifting the logarithmic distribution to smaller sizes. Areas with more abundant precipitation are likely to experience a higher frequency of condensation attachment to Be-7, this is associated with higher mass particulate thereby shifting the distribution to larger particles sizes (Papastefanou 1996).

Increasing the residence time of Be-7 in the atmosphere increases the values of the particle size distribution. A longer residence in the atmosphere allows for an increase in the number of attachments, thus creating particles of larger mass. The summer months promote atmospheric mixing which allows Be-7 to have a longer residence time shifting the size distribution to larger particles. Papastefanou et.al (1996) discovered a correlation between the size of Be-7 aerosol carriers and the change in the seasons.

2.5 Snake River Plains Be-7

Idaho DEQ has 11-sample stations at 10-different locations around the Snake River Plain. During the 3rd quarter of 2016, a duplicate air sampler was introduced at the Idaho Falls locations to sample in parallel with the already in-place sampler. The air sampling locations that are utilized for Be-7 measurements are:

On-site Locations

- Big Lost River Rest Area
- Experimental Field Station
- Sand Dunes Tower
- Van Buren Avenue

Boundary Locations

- Atomic City
- Howe
- Monteview
- Mud Lake

Distant Locations

- Crater of the Moon
- Idaho Falls (HVP 3804)
- Idaho Falls duplicate (HVP 4304)

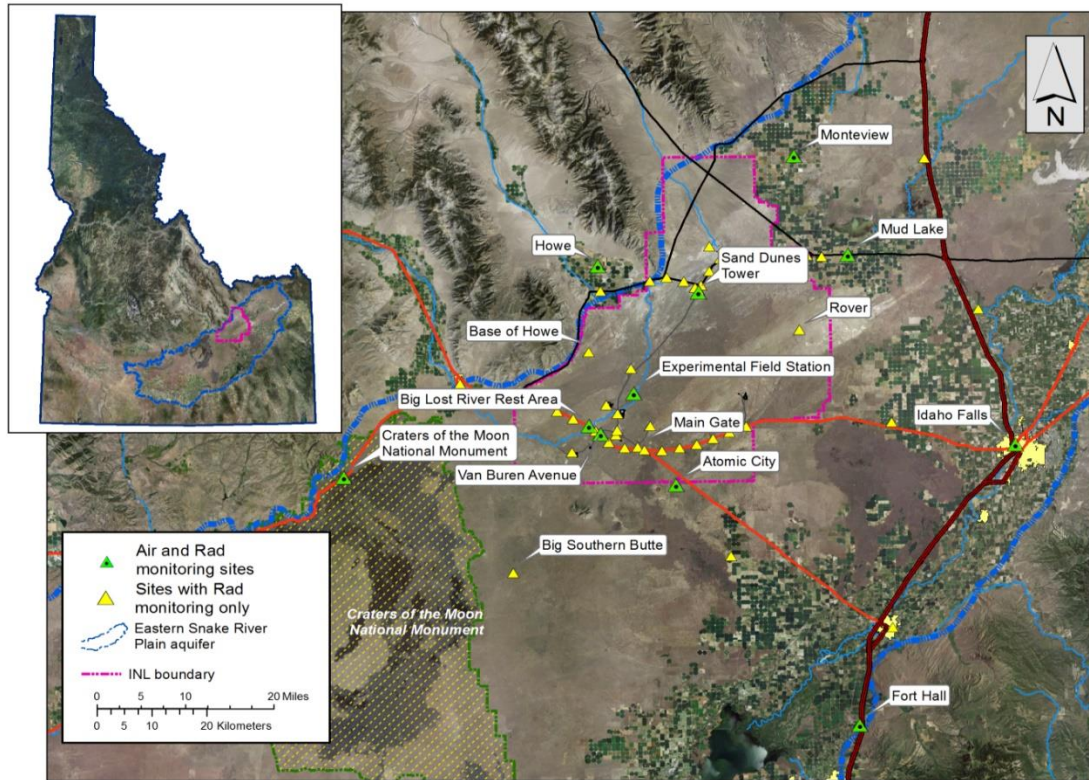


Figure 4. Snake River Plains Sampling Locations (Idaho DEQ Air and Precipitation Monitoring Results)

Table 2.1. Sampling location latitudes and elevation

Location	Elevation (feet)	Latitude
Idaho Falls	4,741	43.514
Mud Lake	4,790	43.841
Monteview	4,793	43.972
Sand Dunes Tower	4,800	43.788
Howe	4,820	43.783
Experimental Field Station	4,940	43.584
Atomic City	5,013	43.445
Big Lost River Rest Area	5,040	43.522
Arco	5,325	43.636
Craters of the Moon	5,897	43.275

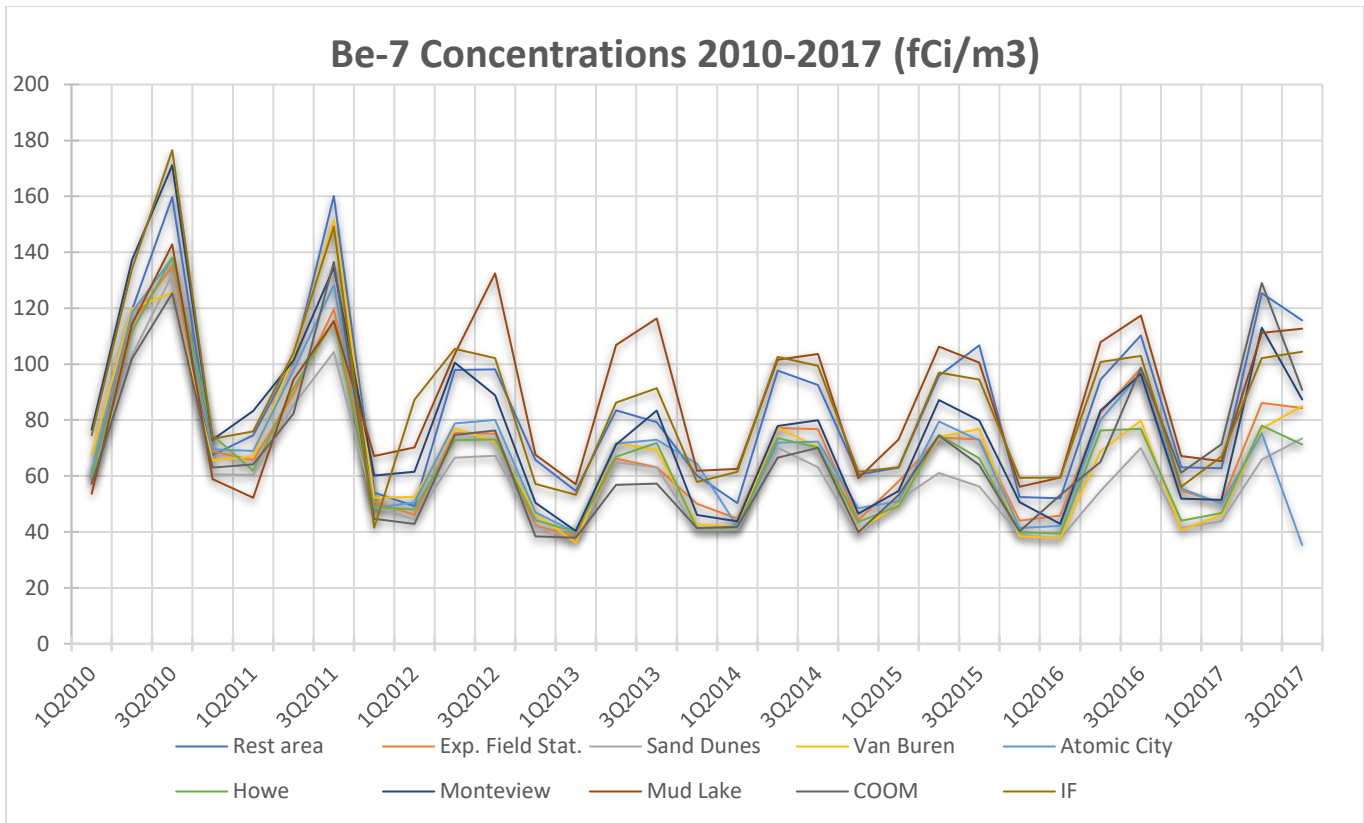


Figure 5. Chart of reported Be-7 concentrations of air from Idaho DEQ in fCi/m³. 11 sampling locations quantified quarterly for the period of Jan.2010 to Sept. 2017.

Figure 5 illustrates the trend analysis of the Snake River Plains sample stations. Average concentrations during 2010 are the highest of the illustrated period and 2014 exhibits the lowest concentration. When compared to Figure 6, it is apparent that the number of sunspots during solar cycle 23, the solar activity minimum, is consistent with the highest Be-7 concentrations and the solar activity maximum is consistent with the lowest Be-7 concentrations.

ISES Solar Cycle Sunspot Number Progression
 Observed data through Feb 2018

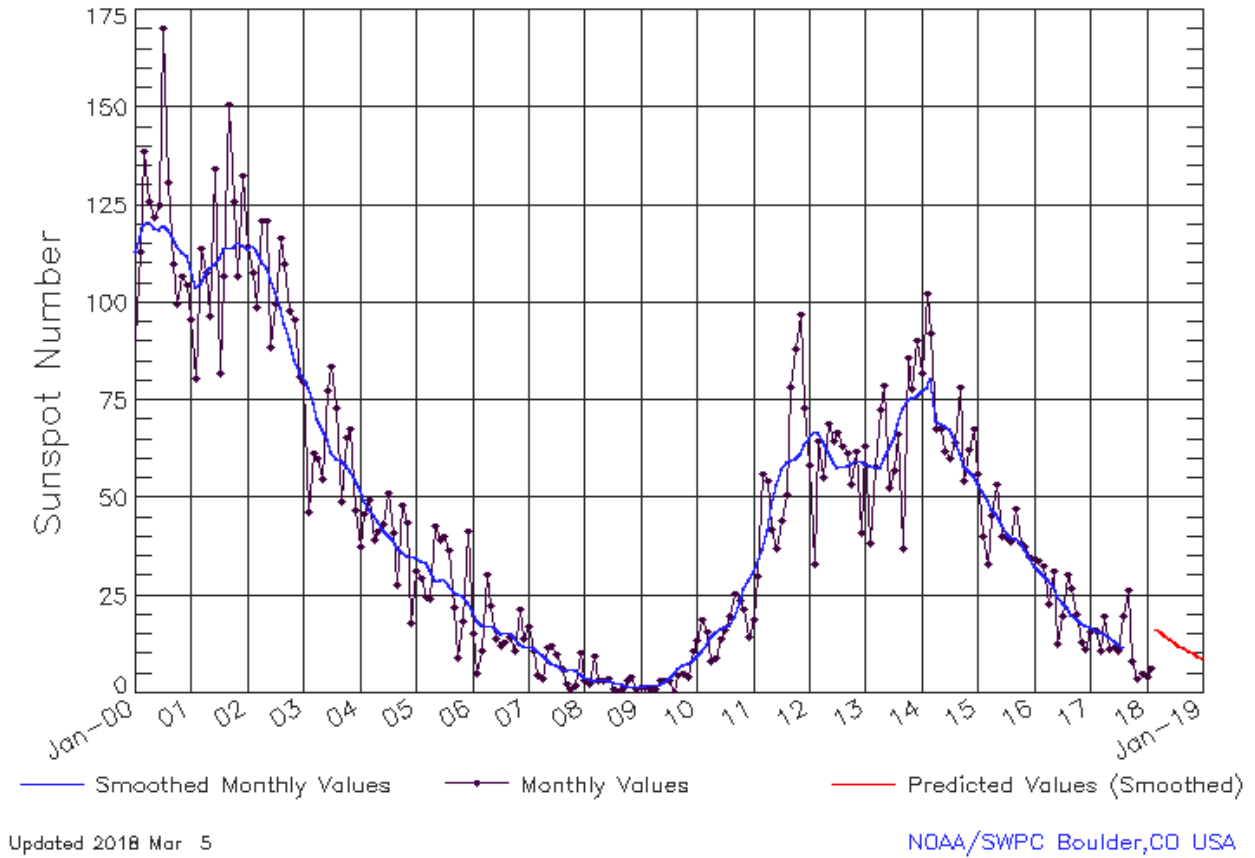


Figure 6. Sunspot activity during solar cycle 22 and 23. (NOAA 2018)

During January 2011, DEQ converted filter media from Versapor-1200® 1.2-µm pore size to Versapor-3000® 3.0-µm pore size. There was no noticeable effect on the collected Be-7 concentrations when compared to previous data and expected values. There was negligible differences in collection efficiency for particles associated with Be-7.

The concentrations of Be-7 reported quarterly from the 11-sample locations over the period of 1st quarter 2010 to 3rd quarter 2017 were compiled and evaluated. The values have units of femto-curies per cubic meter (fCi/m³). The highest concentration reported was 176.5 fCi/m³ in Idaho Falls 3rd quarter 2010. The lowest concentration reported was 35.3 fCi/m³ from Atomic City in 3rd quarter 2017.

The 3rd Quarter 2017 data sheets created by DEQ field Health Physicists note that the Atomic City sampler had some mechanical and power issues. It was observed that on June 1, 2017, the unit tripped a breaker and required restarting. Also during the week of July 13, 2017, power was lost and the system required restarting. The unit lost power again the week of July 27 and August 3. It was noted that on September 27, 2017, the sampling unit was replaced with a new unit. These sampler issues may alter the total sample volume calculated and displayed by the sampler, consequently biasing the actual volume sampled. The error would propagate to the calculated concentrations of Be-7.

2.6 DEQ Sampling Equipment

Idaho DEQ uses the Hi-Q¹ HVP-4304-AFC high volume air sampler. The sampler is a 3-stage, brushless, automatic flow control (variable speed), outdoor 4-inch diameter high volume air sampler designed for continuous use that is housed in a clear-anodized aluminum outdoor shelter. The unit utilizes 115 volts AC, 60 Hz, and 9.0 amps to produce 800 watts of power with a maximum vacuum capacity of 85-inches of water (Hi-Q¹ 2018).

An illuminated LCD displays the flow rate setting, current instantaneous flow rate, total volume of air sampled, and elapsed sample time. The calibrated flow range is between 2 to 15 CFM. The units each weigh 49 pounds and are permanently mounted at each of the 11 sampling locations.

¹ Hi-Q Environmental Products Company. 7386 Trade St. San Diego, CA 92121

The speed of the motor is controlled by a programmable logic controller (PLC) that accepts an input from a mass flow sensor mounted in the sample air stream. The PLC detects changes in the operator's preset flow rate due to changes in temperature, barometric pressure, and pressure-drop due to dust loading on the filter media. The sampler compensates for these changes by adjusting the motor speed to maintain the flow rate setting.

The following equation is used to correct for temperature and pressure difference due to altitude for southeast Idaho:

$$ACF = GasVolume(SCF) \times \left(\frac{273.15}{T}\right) \times \left(\frac{P}{760}\right) \quad (2)$$

Where,

ACF = Corrected sample volume (@ STP)

Gas volume = Total SCF recorded on TSP field data sheet

T = Temperature in degrees Kelvin

P = Pressure in Torr (S.E. Idaho P = 25 inHg = 635 Torr)

*NOAA website indicates the average yearly low of 268 Kelvin (K) and average yearly high of 276K, therefore a yearly average of 272K temperature is negligible when compared to standard temperature of 273.15K and is not included in the calculation.

Therefore,

$$ACF = GasVolume \times \left(\frac{635}{760}\right) = Gas Volume \times 0.835$$

2.7 Filter nomenclature designation

Idaho DEQ designates a formatted nomenclature to identify filters for long term accountability. OP182IHR17 is an example of an assigned nomenclature and the following illustrates the breakdown of the format:

OP – Oversight Program

18 – Last two digits of the year

2 – Calendar quarter

I – Idaho Falls

H – High volume sampler

R – Radiological Sampler

17 – Week number of the year

2.8 Particle collection media

The current air filter media in service is the Versapor-3000® 3- μm pore size, acrylic copolymer membrane on a nonwoven nylon support, with a rated flow rate of 60 LPM / 3.7 cm^2 with a 5-psi differential pressure across the filter (Pall Corporation 2014). The proposed air filter media is the Versapor-5000® 5- μm pore size, acrylic copolymer membrane on a nonwoven nylon support, with a rated flow rate of 88 LPM / 3.7 cm^2 (Pall Corporation 2014). A 4-inch filter has a sampling surface area of 81.07 cm^2 ; therefore, a 3- μm filter is rated for 1314.7 LPM / 46.5 CFM and the 5- μm filter is rated for 1928.2 LPM / 68.1 CFM. The sampler pumps operate well within the capabilities of the filters.

The typical aerosol sampling filters are woven fibrous filters and porous membrane filters. Aerosol filters do not mechanically filter microscopic particles, instead particles collide and attach

to the surface of the filter fibers via the methods of impaction, inertial interception, diffusion, gravitational settling, and electrostatic attraction (Hinds 1999). Gas flow through a porous membrane filter follows an irregular path through a complex pore structure. Particles are removed from the gas stream as they deposit on the structural elements that form the pores. Membrane filters have high removal efficiency ratings and a greater resistance to air flow and pressure drop than other types of filters (Soo 2016). The high efficiency of the porous membrane filters capture aerosol particle sizes much smaller than the manufacturer's indicated pore size, which is based on liquid filtration.

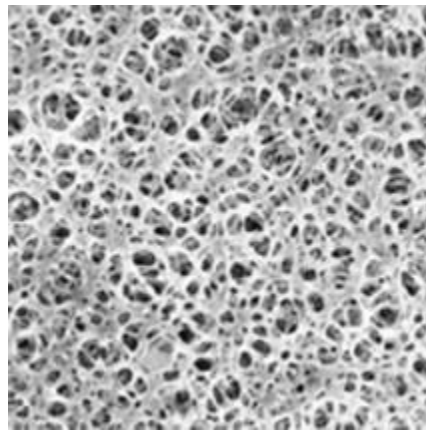


Figure 7. Electron microscope image of Versapor Acrylic Copolymer Membrane Disc Filter (Pall Corporation 2014)

Filters used for sampling are characterized by their ability to collect particulate by determining the efficiency of collection. The fraction of entering particles that are retained by the filter can be expressed as follows:

$$E = (N_{in} - N_{out}) / (N_{in}) \quad (3)$$

Or

$$E = (C_{in} - C_{out}) / (C_{in}) \quad (4)$$

Where N is the number of particulate and C is mass concentration of particulate. Mass concentration is used when evaluating submicron-size particulate and the number of particles are too numerous to count accurately.

Particle penetration decreases exponentially with increasing filter thickness. The easy-to-collect particles are removed primarily in the first few microns of the porous membrane filter. The smaller, more difficult to collect particulate will penetrate farther and be retained deeper in the filter. Particle size distribution changes as the air passes through the membrane for poly-dispersed aerosols.

The structure of the filter creates a resistance to the air flowing, this is called the pressure drop. With respect to a given face velocity, the pressure drop of the filter is directly proportional to the thickness of the filter. The Versapor-3000® and Versapor-5000® have the same volumetric dimensions.

Filter efficiency and pressure drop increase with the accumulation of the collected particles in the filter. The amount of time the filters are used for collection must be considered, due to filters eventually becoming clogged.

The five basic mechanisms by which an aerosol particle can be deposited in a filter are: interception, inertial impaction, diffusion, gravitational settling, and electrostatic attraction. Fiber filters utilize all five mechanisms in contrast to membrane filters that are primarily affected by impaction and interception.

Interception occurs when a particle follows a gas streamline that happens to come within one particle radius of the surface of the particle. The particle hits the surface of the filter membrane and is captured due to its finite size. Pure interception is achieved when the particles follow the

streamlines perfectly by having negligible inertia, settling, or Brownian motion. Interception is the only filtering mechanism by which the particle does not depart from the original streamline.

Inertial impaction occurs when a particle is unable to quickly adjust directions as the direction of the streamline abruptly changes. The Stokes number is the predictive parameter that governs the mechanism of impaction.

Diffusion occurs when Brownian motion causes small aerosol particles to move randomly and disperse within an airstream. Provided the particles contact the surface of the membrane filter, the particle will be collected. Diffusion is a major mechanism when collecting particles 0.1 μm and smaller (Hinds 1999).

Electrostatic attraction occurs when the molecules of the filter have a charge and may attract oppositely charged airborne particles. Charged filter materials can also attract neutral particles by inducing a dipole within the particle and charged particles can be attracted to neutral filter materials.

Sedimentation or gravitational settling occurs when particles fall onto filter materials due to gravitational forces. Sedimentation is generally significant for very large particle, very slow velocities, or if the air is flowing downward into the filter. Due to the sampler housing discriminating particles larger than 2.5 μm , gravitational settling will at most contribute 30% of the total collection efficiency and decreases exponentially for smaller particle sizes (Soo 2016). The particle sizes for Be-7 are too small to consider gravitational settling as an important collection mechanism.

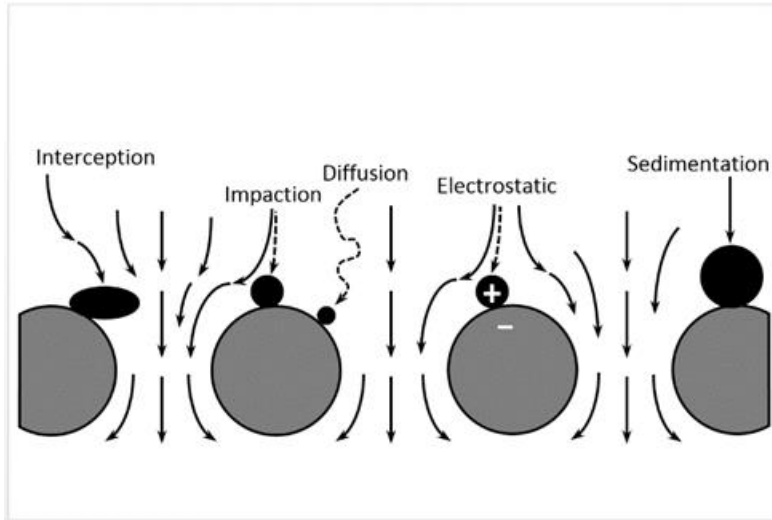


Figure 8. Illustration of aerosol particle collection mechanisms. (Soo 2016)

The effectiveness and relative importance of the collection mechanisms depends on many factors. Higher flow velocities increase the momentum of the particles in comparison to lower flow velocities which allow more time for particulate to diffuse and collect on the filter material. Fibers and particles with irregular shapes or branching structures increase the probability of interception due to the larger surface areas. Figure 9 below illustrates a generalized approach to collection efficiencies based on Hinds et al. 1999 single-fiber efficiency.

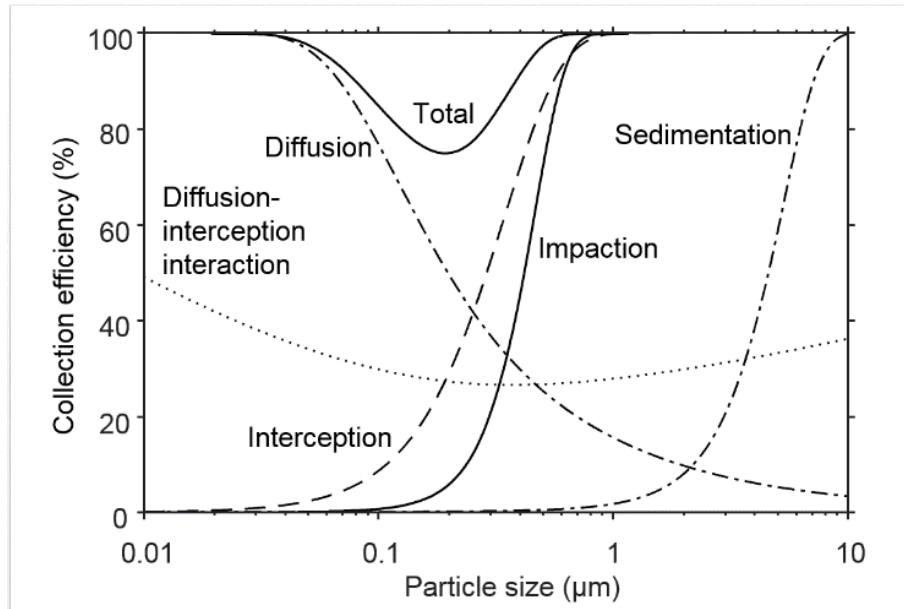


Figure 9. Collection efficiencies of aerosol particle collection mechanisms for a fibrous filter 1mm thick with 2 μ m fibers and air velocity of 10cm/sec. The filter is assumed to be horizontal with air flowing downward onto the surface, enhancing sedimentation. Electrostatic collection is a difficult parameter to quantify and is not shown as a mechanism. (Hinds 1999)

2.9 7-stage cascade impactor

The cascade impactor is an inertial aerosol sampler used to determine the aerodynamic size distribution measurements of aerosols. The aerosol sample is drawn through a series of successively smaller orifices consisting of round holes or jet nozzles with a collection surface placed perpendicular to the direction of flow and very close the exit of each orifice. In each of the 7 stages, the aerosol is accelerated in passage through the stage orifice forcing the particulate to change direction in a 90 degree angle to follow the stream of air flowing through that stage. Particles too large to negotiate the right-angle direction change will impact the collection plate. The impactor stages are designed to provide progressively increasing jet speeds to decrease the cutoff diameter of the average particle size at each stage. The particle size discriminated samples of aerosols collected with the cascade impactor are assessed with respect to the total mass of the

material impacted and retained on the surface of each collection plate (Hinds 1999). Jet nozzle diameter and flow rate are considered when determining the optimum efficiency, precision and accuracy in particle size measurements.

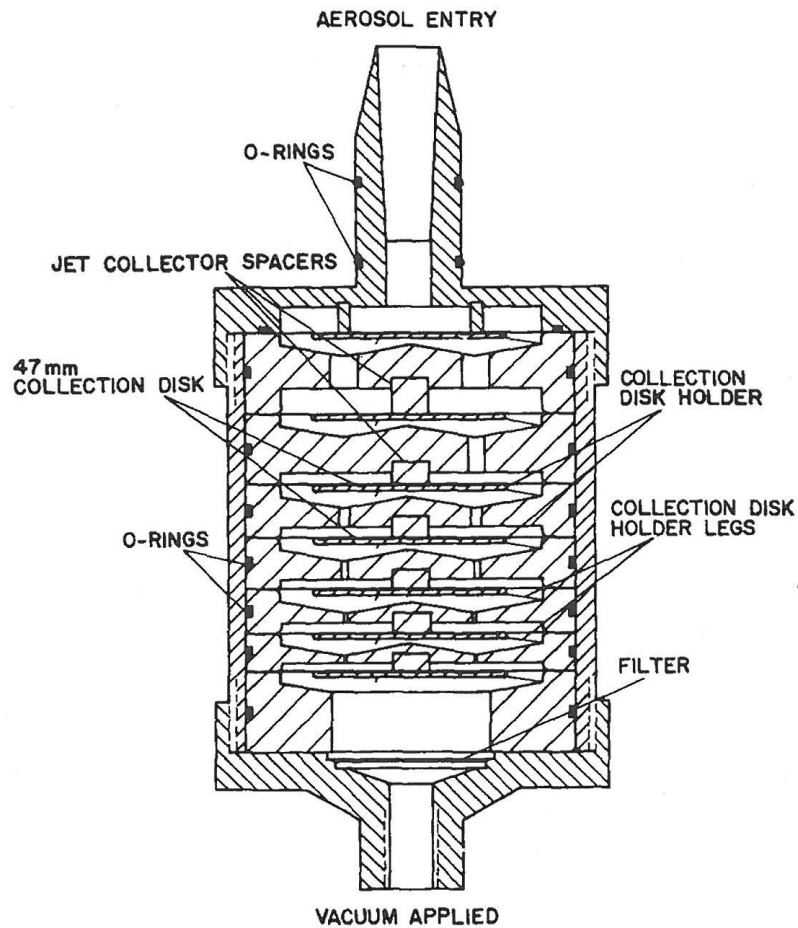


Figure 10. Cross-sectional view of the seven-stage cascade impactor. (Newton 1977)

2.10 HP(Ge)

2.10.1 Semi-conductor detectors

Semi-conductor detectors measure incident ionizing radiation proportional to the number of charge carriers produced per event. Ionizing radiation creates free electrons and electron holes (absence of an electron in the valence band). The combination of the free electrons and electron holes is referred to as an electron-hole pair. The energy required to create an electron hole pair is quantized, therefore the number of electron hole pairs created is proportional to the energy deposited by the incident radiation. Free electrons migrate through the detector's crystal and will move from the valence band to the conduction band provided adequate energy is imparted. The size of the gap between the two bands determines if the material is a semiconductor or an insulator. The larger the gap, the more energy is required for the electrons to jump the gap to the conduction band. (Knoll 2012)

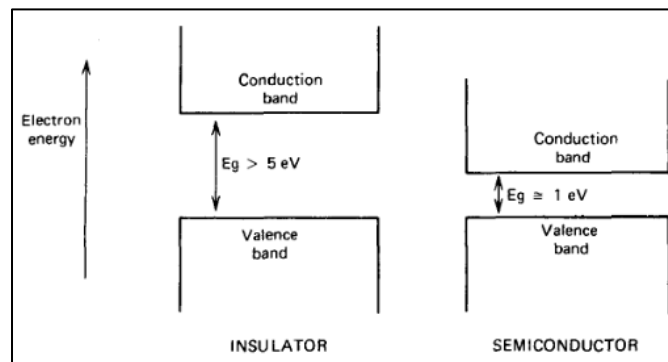


Figure 11. Electron energy requirements of insulator and semiconductor. (Knoll 2012)

A semi-conductor material such as Silicon (Si) or germanium (Ge) crystals require a few electron volts (eV) to create an electron hole pair; compared to a gas-filled detector where approximately 34 eV is required per ionization. More charge carriers are created for the same energy deposited by incident radiation in semiconductor materials.

Si or Ge crystals must be highly purified through the process of zone refining to remove impurities. Si and Ge are in Group IV metals and impurities found are from Group III and Group V. Not all impurities can be removed, and the result is a crystal that is either P-type or N-type. P-type has atoms of elements from Group III in the periodic table such as Boron and Aluminum in the lattice structure, therefore these materials have an atomic structure with one incomplete covalent band, which can be completed by accepting an electron hence they are called acceptor impurities. (Knoll 2012)

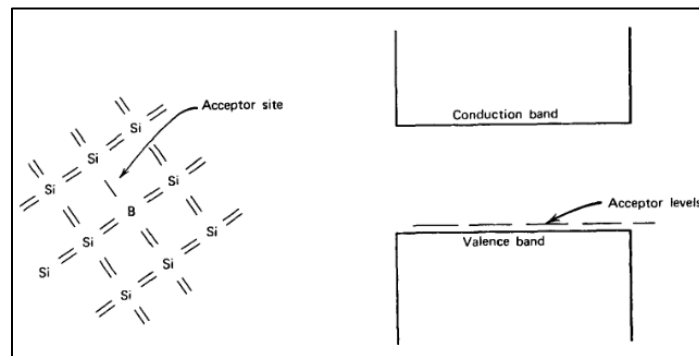


Figure 12. P-type acceptor site. (Knoll 2012)

N-type crystals have impurities from Group V such as Phosphorous and therefore they have one extra electron that may be donated and they are called donor impurities. Acceptor or donor impurities can be compensated for by adding the opposite impurity during the crystal growing process; however, there will still be more of one impurity as it is impossible to create a perfect balance.

Semiconductor material can be arranged within an electrical circuit to allow electron flow in one direction. An n-type contact is formed by implanting a donor ion into the face of the crystal. A p-type face is made on the opposite side by attaching a metallic contact. An n-p junction is therefore created, forming an intrinsic region. The intrinsic region determines the size and

efficiency of the detector. The width between the two faces is the detector volume is known as the depletion region. When a reverse bias voltage is placed across the semiconductor, it causes the charge carriers to move towards their respective polarities as soon as they are developed in the depletion region. The charges collected on the electrodes are integrated by a preamplifier and converted to a voltage pulse.

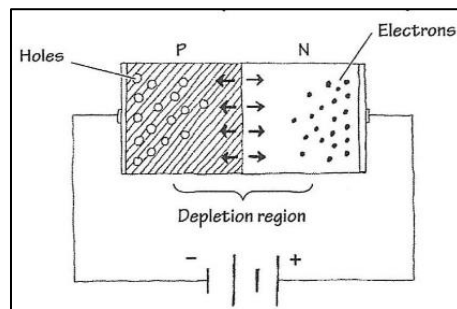


Figure 13. Depletion region and a biased direction of charge carrier flow.

Little energy is required to create an electron-hole pair in a germanium crystal, therefore the crystal must be cooled to the temperature of liquid nitrogen (-196C, -320F) to eliminate the charge carriers produced by heat, thus thermal noise is minimized. The following diagram illustrates a typical germanium detector construction.

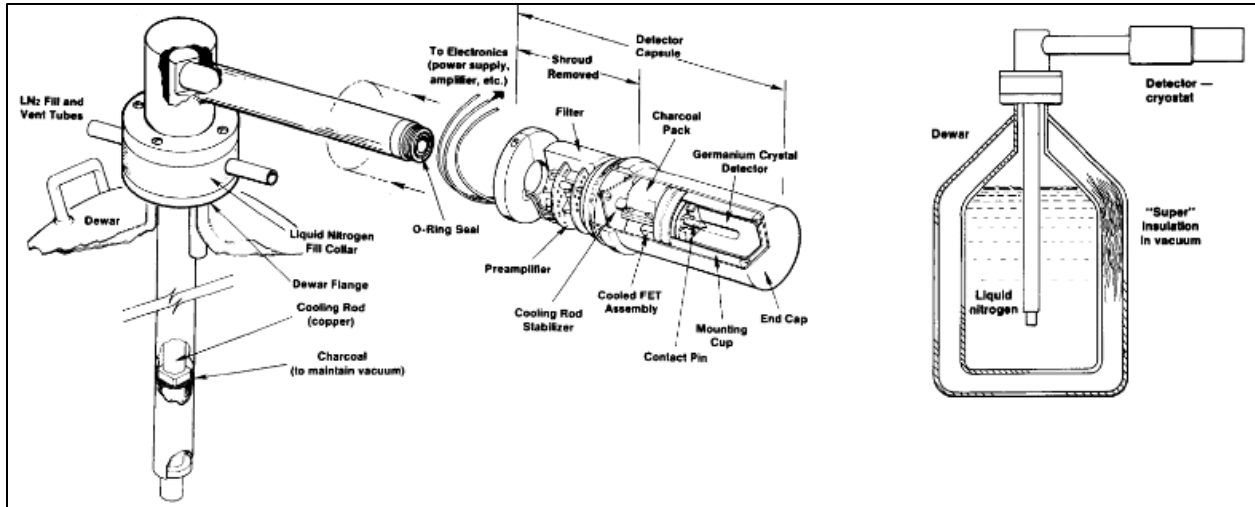


Figure 14. HP(Ge) detector and cryostat unit construction. (Knoll 2012)

2.10.2 Detector calibrations

Energy calibration assigns energy amplitudes to specific channels based on the number of channels available and the range of energy pulses to be observed. A majority of the radionuclides of concern in the nuclear industry emit gamma radiation in the range of 50 keV to 2 MeV. The energy range is then fit over the given number of channels using coarse and fine gain of the amplifier. A source with a known energy signature is then used to manually position the peak and assign energy to a chosen channel. Energy versus channel data is plotted and a best fit line is used to determine the slope of the energy calibration (Knoll 2012). The figure below shows channel 337 being assigned to the 659.28 keV energy peak.

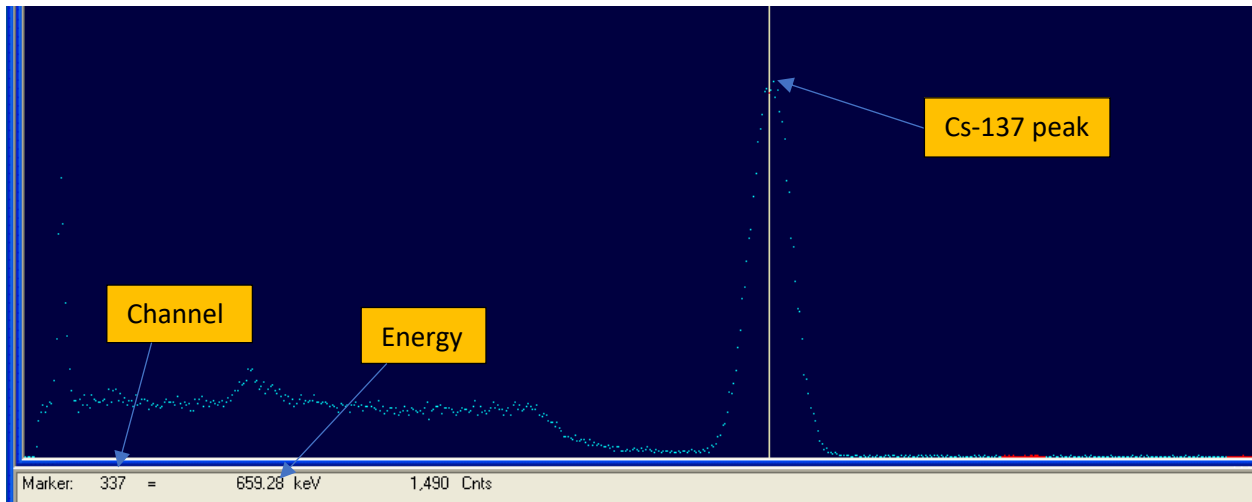


Figure 15. Cs-137 full-energy peak assigned to Channel 337. (Instrumentation Lab 2018)

Efficiency calibration is performed to measure the detector’s collection capability of the source-emitted radiation based on the number of counts in each full energy peak of the spectrum. The efficiency is a ratio of the photons measured by the detector to the photons emitted. The following equation is used to determine efficiency of each energy signature.

$$\epsilon = \frac{NCR}{A(Y)} \quad (6)$$

Where,

NCR = net count rate under each peak

Y = Photon yield

A = Activity of the source

$$A = A_0 e^{-\lambda t} \quad (7)$$

Chapter 3: Materials and Methods

3.1 Materials

ORTEC¹ Gem-Top High Purity Germanium Gamma Detector

- Model number: GEM-90215-P
- S/N:35-TP40640A
- High voltage 2500V Positive.
- 100% relative efficiency

Eckert & Ziegler² Multi-nuclide Source.

- 5.124 μ Ci total activity
- Serial number: 1973-32-3
- Created: 10/1/2017
- EML S/N: RS48647

HI-Q³ High Volume Total Suspended Particulate (TSP) Continuous Sampler

- Model number: 4304-AFC-BRL-KIT
- Serial Number: 21256

HI-Q³ High Volume Total Suspended Particulate Continuous Sampler

- Model number: HVP-3804AFC
- Serial Number: 9011

Hi-Q³ 4-inch filter cartridge

- CAT#: RVPH-201

Pall⁴ Versapor-5000R® 5- μ m copolymer membrane filter

Pall⁴ Versapor-3000R® 3- μ m copolymer membrane filter

In-Tox⁵ 7-stage cascade impactor

- Model D

Canberra⁶ Amplifier

- Model: 9615

Canberra⁶ High Volt Power Supply

- Model: 9645

¹ Advanced Measurement Technology, 801 South Illinois Avenue Oak Ridge, Tennessee 37830

² Eckert & Ziegler Isotope Products, 24937 Ave Tibbitts, Valencia, CA 91355

³ Hi-Q Environmental Products Company, 7386 Trade St. San Diego, CA 92121

⁴ Pall Corporation 25 Harbor Park Dr, Port Washington, NY 11050

⁵ In-Tox Products, LLC, 101 Wilderness Ct. S., Moriarty, NM 87035

⁶ Canberra Industries, 800 Research Pkwy, Meriden, CT 06450

General Electric¹ Suction Pump

- Model: 5KC43MG2625X
- ½ HP, 60 HZ, Continuous run

Sierra² mass flow rate meter

- Model: 826-NX-OV1-PV1-V1
- S/N: 121861
- Range: 0-60 liters per minute (LPM)
- Readability: 0.1 LPM
- Calibrated: 6/4/2018

Ohaus³ Scale

- Model: AR2140
- Serial Number: H0411202351092
- Readability: 0.0001g

3.2 Experiment I: Side-by-side filter collection efficiency comparison

3.2.1 HP(Ge) calibration

The high purity germanium (HP(Ge)) detector high voltage supply was set to 2500V per manufacturer specifications. Coarse gain was set to 25. Fine gain was set at 1.4810.

Energy and efficiency calibrations were performed using the NIST traceable multi-nuclide source. 8192 channels were used providing a 0.25 keV per channel resolution.

A 24-hour background was performed as a baseline and to lower the Be-7 minimum detectable activity (MDA).

¹ General Electric Company, 3135 Easton Turnpike, Fairfield, CT 06828

² Sierra Instruments, 5 Harris Court, Building. L Monterey, CA 93940

³ Ohaus Corporation 7 Campus Drive, Suite 310 Parsippany, NJ 07054 USA

3.2.2 Obtaining the samples

A 5- μm and 3- μm filter were used for the parallel sampling experiment in the two Idaho Falls samplers at the same location for 3 sampling weeks (4/19/18 to 4/26/18, 5/24/18 to 5/31/18, 5/31/18 to 6/7/18). A 3- μm filter was used in the normal Idaho Falls sampler and 5- μm was used in the duplicate sampler. Both samplers sampled continuously for 168 hours each week.

Prior to placing a new filter on the sampler, the unused filter's mass was measured, and the sample designator was written on the filter's edge. The sample filters were handled with tweezers to prevent human skin contaminants, and thus avoiding the addition of mass to the filter which may result in erroneous results when determining the final mass. The filters are again weighed and after removal; total mass, sample time, volume sampled, and flow rate are logged. Each filter was kept in storage for 5 days in a desiccant material to allow short-lived radon decay product radionuclides to decay and remove any residual moisture.

OP182IHR17DP was a 5- μm filter used on the duplicate sampler. The filter was placed in service 4/19/18. Total sample time was 168.2 hours. Total volume sampled 2,052 m^3 . The mass accumulated from the atmosphere was measured to be 0.0902 ± 0.001 mg. The average sampling rate was 7.2 ± 0.1 CFM.

OP182IHR17 was the normal 3- μm filter used on the designated Idaho Falls air sampler. The filter was placed in service 4/19/18. Total sample time 168.2 hours. Total volume sampled 2,054 m^3 . The mass accumulated from the atmosphere was measured to be 0.0428 ± 0.001 mg. Average sampling rate was 7.2 ± 0.1 CFM.

OP182IHR22DP was a 3- μm filter used on the duplicate sampler. The filter was placed in service 5/24/18. Total sample time was 166.4 hours. Total volume sampled was 2,030 m^3 . The

mass accumulated from the atmosphere was measured to be 0.0397 ± 0.001 mg. Average sampling rate was 7.2 ± 0.1 CFM.

OP182IHR22 was a 5- μ m filter used on the designated Idaho Falls air sampler. The filter was placed in service 5/24/18. Total sample time was 166.3 hours. Total volume sampled was 2,032 m³. The mass accumulated from the atmosphere was measured to be 0.0388 ± 0.001 mg. Average sampling rate was 7.2 ± 0.1 CFM.

OP182IHR23DP was a 3- μ m filter used on the duplicate sampler. The filter was placed in service 5/31/18. Total sample time 170.1 hours. Total volume sampled was 2,076 m³. The mass accumulated from the atmosphere was measured to be 0.0424 ± 0.001 mg. Average sampling rate was 7.2 ± 0.1 CFM.

OP182IHR23 was a 5- μ m filter used on the designated Idaho Falls air sampler. The filter was placed in service 5/31/18. Total sample time 170.3 hours. Total volume sampled was 2,080 m³. Mass accumulated from the atmosphere was determined to be 0.0435 ± 0.001 mg. Average sampling rate was 7.2 ± 0.1 CFM.

3.2.3 Analyzing the samples

Each filter was placed in the 4-inch plastic sample holder and analyzed for 86,400 sec (24hr). A standard HP(Ge) in a copper-lined, lead shield was used for analysis.

3.2.4 Filters in series

An additional experiment involved two filters sampled in series. A 6-inch, PVC series sampling apparatus was used allowing the two filters to sample in series. The apparatus mounts vertically to the normal sampling suction forcing air to be passed through the top most filter first,

traveling through the volume of the apparatus and finally through the second filter. The 3- μm filter was placed in the normal sampling position of the TSP sampler as the second filter in the series. The 5- μm filter was placed on top of the apparatus allowing the sampled air to first pass through the 5- μm filter. The particles not collected by the 5- μm filter would then pass through and allow the 3- μm filter an opportunity to collect the particles. Due to the construction of the apparatus and the sampling rate, the probability of gravitational settling increases as a mechanism of collection on the second filter in the series.

The purpose of this experiment was to compare collection efficiencies of the 5- μm filter and the 3- μm filter. The particles collected by the 3- μm filter are those that were not collected by the 5- μm filter. This experiment was not intended to be a stand-alone hypothesis test, rather supporting data to the comparison of the efficacy of the two filters.

The apparatus was placed on the duplicate TSP sampler (Model number: 4304-AFC-BRL-KIT) during the week of 5/10/18 to 5/17/18. Total hours sampled was 160.3 hours. Total volume sampled was 1958 m^3 . Average sampling rate was 7.2 ± 0.1 CFM. The following figure is the series sampler with the 5- μm on top and the 3- μm filter on the bottom:



Figure 15. Series sampling apparatus

3.3 Experiment II: Particle size discrimination of the 5- μ m filter

The 47-mm aluminum collection plates and the final stage 47-mm membrane filter were individually weighed on the scale prior to assembling the cascade impactor. The last stage was placed in the impactor housing first and each stage was placed in the housing in descending order each with its own aluminum collection plate. No oils or fluids were used to improve the particle collection.

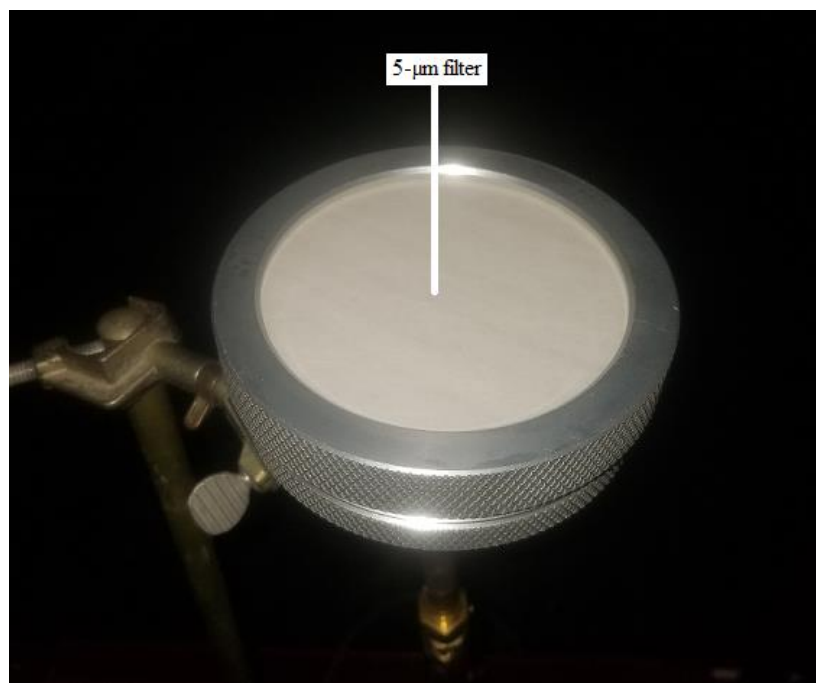


Figure 16. Versapor-5000® 5- μ m filter in an aluminum sampling cartridge.

The 5- μ m filter was placed in a 4-inch filter aluminum cartridge, as seen above in Figure 16, and placed at the air intake of the sampling setup. A Tygon® hose, 12 inches in length and 0.5 inches inside diameter, was used to connect the filter cartridge to the inlet of the cascade impactor. Both the filter cartridge and the cascade impactor were vertically mounted, using a stand, to maximize particle collection and minimize deposition of particles on the inside walls of the Tygon® hose as air flowed to the cascade impactor.

The exhaust of the cascade impactor then flowed through a length of 0.25 inch diameter hose to the mass flow-rate meter. The exhaust line of the mass flow rate meter was connected to the inlet of the rotameter. The exhaust of the rotameter was connected to the suction pump. The suction was energized and the flow valve controller was used to adjust the flow rate to 28.3 ± 0.5 LPM (1 CFM) as read on the flow rate meter digital display.

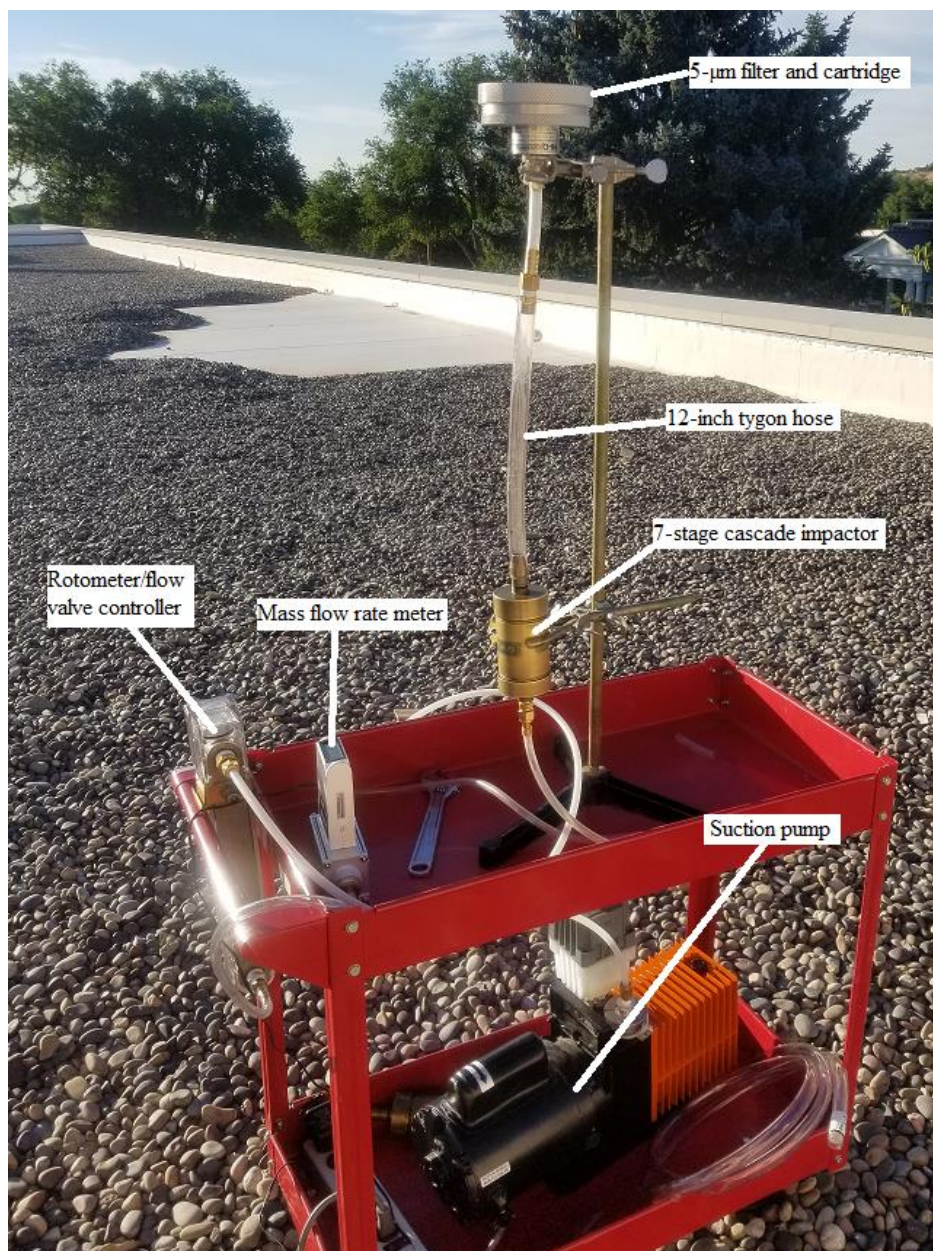


Figure 17. Experiment III final sampling setup on the roof of the Physical Science Building Pocatello, ID.

Figure 17 above shows the experiment set up with each portion of the sampling line. The cascade impaction apparatus was set up on the roof of the Physical Science Building (Bldg. 3) at Idaho State University in Pocatello, ID (latitude – 42.5N, elevation – 4,462ft). The sample started at 16:10 on 6/25/18 and ended at 10:30 on 6/27/18 for a total of 42.33 hours. During the time of sampling, it did not rain nor were there abnormal conditions that would have influenced the results of the experiment.

3.4 Experiment III: Filter recount as a composite

Each 3- μ m and 5- μ m filter used in Experiment I was reanalyzed on the same detector for the same count time of 86,400sec with 12 unused-filter papers stacked under the filter for comparison. The stack of filters replicates the normal counting method of the quarterly composite of 13 air filters and represents a “worst case” where all the activity is on the filter which is furthest from the detector and subject to the most attenuation.

Chapter 4: Results and Discussion

All activities of samples measured by HP(Ge) gamma detection were decay corrected to the time of sample acquisition from their respective sampling apparatuses.

4.1 Experiment I: Side-by-side filter collection efficiency comparison

Table 4.1: Idaho Falls normal and duplicate sampler results

Filter collection date	Volume sampled (m ³)	Elapsed Time (hrs)	Mass (mg)	Filter pore size (μm)	Total Activity (pCi)	Uncertainty (pCi)	MDA (pCi)
4/26/2018	2052	168.2	0.0902	5	549.4	68.7	56.2
4/26/2018	2054	168.2	0.0428	3	604.5	70.0	55.3
5/31/2018	2032	166.3	0.0388	5	386.5	38.4	48.7
5/31/2018	2030	166.4	0.0397	3	551.6	50.0	58.0
6/7/2018	2080	170.3	0.0435	5	426.1	43.6	52.9
6/7/2018	2076	170.1	0.0424	3	561.6	51.3	54.9

During the week of 4/19/18 to 4/26/18, the 5-μm filter collected $90.9 \pm 15.5\%$ of the total Be-7 activity collected by the 3-μm filter.

During the week of 5/24/18 to 5/31/18, the 5-μm filter collected $70.1 \pm 11.3\%$ of the total Be-7 activity collected by the 3-μm filter.

During the week of 5/31/18 to 6/7/18, the 5-μm filter collected $75.9 \pm 10.4\%$ of the total Be-7 activity collected by the 3-μm filter.

The 5- μm filter consistently resulted in an activity less than the 3- μm filter. The mean value of the collection efficiency of the 5- μm compared to the 3- μm is $78.9 \pm 12.6\%$. All calculated activities are above minimum detectable activity (MDA) for Be-7.

The results suggest a rejection of the null hypothesis; the 5- μm does not display a comparable collection efficiency of Be-7 activity to that of the 3- μm filter. The differences in the volumes sampled and elapsed time are not significant enough to explain the difference in activity.

When considering the masses collected, the 5- μm filter was consistent with that of the 3- μm suggesting smaller particles with less mass, in the range of 0.4- μm to 1.2- μm for Be-7, did not affect the total mass but may not be collected as efficiently by the 5- μm filter size.

The 3- μm filter results, when compared to each other, resulted in a mean value of 572.6 ± 57.8 pCi and a standard deviation of 28.1 pCi. The 5- μm filter results, when compared to each other, resulted in a mean value of 454.0 ± 51.9 pCi and a standard deviation of 85.0 pCi.

4.1.1 Filter in series

Initial and final masses of the filters were not determined, thus data is exclusive to Be-7 activity. The following table compares Be-7 activities of the filters in series:

Table 4.2: 5- μm and 3- μm in-series samples.

Filter	Total Activity (pCi)	Uncertainty (pCi)	MDA (pCi)	Fraction of total activity (%)
3-μm	70.65	38.84	46.6	$12.8\% \pm 7.1$
5-μm	481.6	51.05	61.4	$87.2\% \pm 13.6$

The data suggests that the 5- μm filter is $12.8 \pm 7.1\%$ less efficient at collecting Be-7 aerosols than the 3- μm filter.

4.2 Experiment II: Particle size discrimination of the 5- μm filter

The 4-inch, 5- μm membrane filter was removed and weighed for total mass accumulated. Initial mass was 0.553 g, final mass 0.569 g, total mass accumulated on the filter was calculated to be 0.016 ± 0.0001 g. The cascade impactor was disassembled and each stage collection plate was weighed for total mass accumulated. The total mass collected by the cascade impactor was 0.0035 ± 0.0001 g and distributed among the collection plates and the last filter. The total mass accumulated by the filter and cascade impactor was 0.0195 ± 0.0001 g. The 4-inch, 5- μm filter collected $82.05 + 0.63\%$ of the sampled particulate mass. The cascade impactor collected $17.95 + 2.9\%$ of the sampled particulate mass. The following table is a breakdown of the mass collected by the cascade impactor:

Table 4.3: Cascade impactor mass by stage.

Collection plate (stage#)	Initial Mass (g)	Final mass (g)	Fraction of total mass of cascade impactor	Size range (μm)
1	0.0446	0.0446	0.0%	>12
2	0.0447	0.0447	0.0%	7-12
3	0.0447	0.0447	0.0%	4-7
4	0.0446	0.0446	0.0%	2.5-4
5	0.0442	0.0442	0.0%	1.6-2.5
6	0.0446	0.0446	0.0%	1.0-1.6
7	0.0446	0.0450	11.4%	0.6-1.0
last filter (3-μm)	0.0726	0.0757	88.6%	<0.6

The 5- μm filter is observed to have a collection efficiency of 100% for particles as small as 1.0- μm . 2.1% of the total mass (0.0195g) is attributed to particles in the size range of 0.6- μm to 1.0- μm . 15.9% of the total mass is attributed to particles smaller than 0.6- μm .

Without knowing the particle size distribution of an unfiltered atmospheric sample, the collection efficiency of the 5- μm filter cannot be quantified for particles smaller than 1.0- μm . The particles collected by the cascade impactor does not imply the 5- μm filter did not collect some percentage of those particle sizes.

The 47-mm Versapor-3000® filter, used as the last stage to collect particles smaller than 0.6- μm , was analyzed for radionuclide identification to assess the presence of Be-7. Be-7 was not identified in the analysis. Naturally occurring Pb-212 and Bi-214 were detected. This indicates that the particles not collected by the 5- μm filter, smaller than 0.6- μm , did not have a Be-7 concentration high enough to be detected on the HP(Ge).

4.3 Experiment III: Filter recount as a composite

Table 4.4. Single filter activity versus composite recount activity.

Sample designator	Filter Collection date	Filter size (µm)	Single Filter Activity (pCi)	Uncertainty (pCi)	MDA (pCi)	Composite Activity (pCi)	Uncertainty (pCi)	MDA (pCi)
OP182IHR17DP	4/26/2018	5	549.4	68.7	56.2	452.2	55.6	29.7
OP182IHR17	4/26/2018	3	604.5	70.0	55.3	361.3	58.9	87.3
OP182IHR22	5/31/2018	5	276.3	36.7	51	254.8	38.0	55.4
OP182IHR22DP	5/31/2018	3	551.6	50.0	58	267.6	37.0	53.4
OP182IHR23	6/7/2018	5	365.0	40.9	51.7	363.6	28.9	19.1
OP182IHR23DP	6/7/2018	3	529.2	49.6	53.1	478.2	36.3	19.9

OP182IHR17DP composite recount resulted in $82.3 \pm 14.4\%$ of the single filter count.

OP182IHR17 composite recount resulted in $76.7 \pm 13.7\%$ of the single filter count.

OP182IHR22 composite recount resulted in $96.4 \pm 14.6\%$ of the single filter count.

OP182IHR22DP composite recount resulted in $89.3 \pm 10.6\%$ of the single filter count.

OP182IHR23 composite recount resulted in $85.3 \pm 12.1\%$ of the single filter count.

OP182IHR23DP composite recount resulted in $90.3 \pm 12.0\%$ of the single filter count.

All composite recounts resulted in a lower calculated Be-7 activity. The mean of the composite recount loss in calculated activity is $86.7 \pm 12.9\%$. The data suggests that there is a loss of calculated activity of approximately $13.3 \pm 3.6\%$, of the top-most filter, when counting as a 13-filter composite. The hypothesis is rejected due to the composite activity is consistently less than the single filter activity.

The experiment performed during the 3rd quarter of 2016 observed a 20.8% loss of activity as a composite analysis when compared to the single filter analysis.

Chapter 5: Conclusions and future work

This research has illustrated the trade-off of collection efficiency of the filter media and reliability and longevity of the sampling units. The Be-7 concentrations in the Snake River Plains reported have shown to follow a calculated trend and are consistent with reported data world-wide. DEQ's field sampling units exhibit reliability in continuous sampling, and to ensure a greater percentage of the aerosols associated with Be-7 are collected, the continued use of the Versapor-3000® 3- μm filter is recommended.

The side-by-side comparison of filter efficiency indicates the 5- μm filter collects approximately $78.9 \pm 12.6\%$ when compared to the 3- μm filter. The series sampling suggests the 5- μm filter collects approximately $87.2 \pm 7.1\%$ of the activity collected by the 3- μm filter. The composite recount suggests a decrease in counting efficiency of approximately $86.7 \pm 12.9\%$ when compared to filters analyzed on the face of the detector. The cascade impactor characterized the unfiltered particulate of the 5- μm filter as $<1.0\text{-}\mu\text{m}$ with the majority of the particles $<0.6\text{-}\mu\text{m}$ in size.

To completely quantify the 5- μm collection efficiency of submicron particles, the cascade impactor must be used to create a particle size distribution of an unfiltered atmospheric sample.

More data sets are required to accurately determine the collection efficiency of the 5- μm filter.

References

- Bas M, Ortiz J, Ballesteros L, Martorell S. Analysis of the Influence of Solar Activity and Atmospheric Factors on Be-7 Air Concentrations by Seasonal-trend Decomposition. *Atmospheric Environment*. 145 pp.147-157, 2016.
- DEQ-INL OP, Air Monitoring and Precipitation Results. 2010-2017
- Doering C. Measurements of the Distribution and Behavior of Beryllium-7 in the Natural Environment, Queensland University of Technology, pp.4; 2007.
- Feely H W, Larsen R, Sanderson C. Factors that cause Seasonal Variations in Beryllium-7 Concentrations in Surface Air. *Journal of Environmental Radioactivity* 9, pp. 223-249. 1989
- Giraud L., Hart G., Peterson B., Nakata T., 9th Annual Meeting of the Northwest Section of the APS, Volume 52 2007, Pocatello, ID.
- Hinds W C. Aerosol Technology: Properties, Behavior, and Measurement of Airborne Particles, Second Edition. 1999
- Jiwen L, Starovoitova VN, Wells DP. Long-term variations in the surface air ⁷Be concentration and climatic changes. *Journal of Environmental Radioactivity*. 2013-116: pp. 42-47
- Kotsopoulou E, Ioannidou A. Be-7 Atmospheric Concentration at Mid Latitudes (40°) during a year of solar minimum. Aristotle University of Thessaloniki. EPJ Web of Conferences 24; EDP Sciences 2010
- Lindsley W G. Filter Pore Size and Aerosol Sample Collection. NIOSH Manual of Analytical Methods (NMAM), 5th Edition; 2016
- Newton G J, Raabe O G, Mokler B V. Cascade Impactor Design and Performance. Inhalation Toxicology Research Institute, Lovelace Foundation. 1977
- NOAA Space Weather Prediction Center. ISES Solar Cycle 24 Sunspot Number Progression. Solar Cycle Progression. May 7 2018. <https://www.swpc.noaa.gov/products/solar-cycle-progression>
- Pall Corporation. Versapor Acrylic Copolymer Membrane Disc Filter Data Sheet. 2014
- Papastefanou C, Ioannidou A, Beryllium-7 Aerosols in Ambient Air, *Environmental International*, Vol. 22, Suppl. 1, pp. S125-S130, 1996
- Poluianov S V, Kovaltsov GA, Mishev AL, Usoskin IG. Production of cosmogenic isotopes ⁷Be. 2016.
- Rez AK. Spallation Reaction Physics. *Fac Nucl Sci Phys Eng Czech Tech Univ Prague*. 2010. <http://ojs.ujf.cas.cz/~krasa/ZNTT/SpallationReactions-text.pdf>.

- Soo J, Monaghan K, Lee T, Kashon M, Harper M. Air Sampling filtration media: Collection Efficiency for respirable size-selective sampling. *Aerosol Science Technology*. Jan 2016; 50(1): 76-87.
- Talpos S, Rimbu N, Borsan D. Solar forcing on the Be-7 air concentration variability at ground level, *Journal of Atmospheric and Solar-Terrestrial Physics* 67. 2005; October 2005, 1626-1631
- Terzi L, Kalinowski M. World-Wide Seasonal Variation of Be-7 Related to Large-scale Atmospheric Circulation Dynamics. *Journal of Environmental Radioactivity*. 2017; 178-179:1-15

Appendix I. DEQ reports 2010-2017 in fCi/m³(1x10⁻³pCi/m³)

	REST AREA	EFS	SAND DUNES	VAN BUREN	ATOMIC CITY	HOWE	MONTEVIEW	MUD LAKE	COTM	IF
1Q2010	59.1	57.1	60	67.7	61.2	59.7	76.5	53.6	57.3	74.5
2Q2010	119.3	115.2	103	119.9	118.4	111.6	137.2	114.2	101.9	133.9
3Q2010	159.7	135	132	125.6	138	138.1	171.1	142.8	125.3	176.5
4Q2010	67.4	68.8	60.6	65.6	69.5	74.5	72.9	58.9	63	73.3
1Q2011	74.5	65.6	60.3	66.9	68.9	61.8	83.2	52.2	64.1	75.9
2Q2011	101.6	89.2	85.4	102.6	97.8	91.4	101.3	94.4	82.3	103.9
3Q2011	160.1	119.6	104.3	151.6	128.2	115.5	134.6	115.3	136.5	149.2
4Q2011	54	50.8	48.9	52.2	48.6	48.9	60.1	67.1	44.7	41.5
1Q2012	49.2	46.1	44.5	52.5	50.5	48	61.5	70.2	42.8	87.3
2Q2012	97.9	75.4	66.5	77.1	78.8	72.8	100.5	103.6	74.7	105.5
3Q2012	98.1	75.1	67.2	72.3	80	73	88.8	132.5	76.3	102.1
4Q2012	65.7	42.3	41.8	46.6	47	44.2	50.4	67.6	38.4	57.1
1Q2013	54.6	38.1	37.3	36	39.9	40	40.3	57	37.9	53.3
2Q2013	83.5	66.2	64.9	71.8	71.6	66.9	71.2	106.8	56.8	86.2
3Q2013	79.2	63.1	63	69.3	72.9	71.8	83.4	116.3	57.3	91.4
4Q2013	60.1	50.1	40.8	42.6	64.4	41.2	46	61.8	41.3	57.8
1Q2014	50.3	44.7	40.8	41.8	41.9	41.5	43.8	62.5	41.8	61.5
2Q2014	97.7	77.2	70.1	77.3	71.9	73.5	77.9	101.5	66.5	102.6
3Q2014	92.5	76.7	63.1	70.3	72.3	70.2	79.9	103.6	70.1	99.4
4Q2014	60.5	44.2	38.6	40.4	48.5	43.5	46.5	59.2	39.9	61.5
1Q2015	63	58.1	51.3	49.9	51	49.2	54.6	73.1	53.1	63.1
2Q2015	95.8	73.7	61	73.8	79.5	74.7	87.1	106.3	74.4	97
3Q2015	106.7	73.1	56.2	76.8	72.7	66.3	79.8	100.5	63.9	94.4
4Q2015	52.5	44	38.8	38.4	41.4	39.9	50.6	56.1	40.2	59.3
1Q2016	52	45.8	37.6	37.7	42.1	39.4	42.8	59.4	53.1	59.4
2Q2016	94.5	82.5	54.6	68.8	80	76.3	83.3	107.8	65.1	100.7
3Q2016	110.3	98.5	70	79.8	96.8	76.8	96.5	117.4	98.7	102.9
4Q2016	63.1	54.7	41.4	40.6	55.5	44	51.9	67.1	61.1	56.1
1Q2017	62.7	50.4	43.9	46.1	50.1	46.7	51.4	65.3	71.3	67
2Q2017	125.3	86.1	65.9	76.9	75.2	78	113	111.2	129	102.1
3Q2017	115.6	84.3	73.4	85	35.3	71.2	87.4	112.7	90.8	104.4

